

Time-dependent Quantum Scattering Calculation of the $O(^3P)+HBr(DBr)$ Reaction*

ZUO, Guo-Ping^{1,2} TANG, Bi-Yu^{1,2} HAN, Ke-Li³

(¹Department of Physics, Xiangtan University, Xiangtan 411105; ²Institute of Modern Physics, Xiangtan University, Xiangtan 411105; ³Center for Computational Chemistry and State Key Laboratory of Molecular Reaction Dynamics, Dalian Institute of Chemical Physics, Chinese Academy of Sciences, Dalian 116023)

Abstract An exact three-dimensional time-dependent quantum wave packet was employed to calculate the $O(^3P) + HBr(DBr)$ reaction using a generalized London-Ering-Polanyi-Sato(LEPS) potential energy surface. The results showed that vibrational excitation is effective for the reaction, and rotational excitation has an orientational effect in definite energy range. The rate constants and the reaction cross sections for the title reactions have been computed, the calculated rate constants k_{O+HBr} agreed well with experimental data. By comparing with relevant results, it can be found that the kinetic isotope effects of the reaction are relatively obvious.

Keywords: Time-dependent quantum wave packet, Rate constants, Reaction cross sections

The reaction



is one of the prototypical hydrogen-atom-transfer reactions and belongs to the heavy-light-heavy reaction class. The reaction is characterized by a very small skewing angle ($\beta=15.6^\circ$)^[1], which promotes approximate conservation of kinetic energy, and the preferential release of the reaction exotherm into product OH vibrational and rotational degrees of freedom. It is expected to manifest important quantum mechanical (QM) effects, such as tunneling and resonances at the transition state^[2-4]. The $O(^3P)+HBr$ reaction is also important as one possible source of retardation in HBr inhibited flames^[5].

In spite of the importance of this reaction class, the $O(^3P)$ reaction with HBr has received much less attention by theorists and experimentalists than the reaction with HCl^[6-13]. The dynamics property of the $O(^3P)+HBr$ reaction has been investigated through the laser pump-probe experiments by McKendrick *et al.*^[14-15], which revealed specific disposal of energy into OH vibrational and rotational excitation, broadly consistent with expectation based on kinematics considerations. Brouard *et al.*^[16] have also investigated the dynamics property of the $O(^3P)$ reaction with HBr using the photon-initiated reaction technique coupled with

Doppler-resolved laser induced fluorescence(LIF) detection. They revealed a detailed angular distribution of the scattered OH products and also suggested that the reaction does not take place on a collinearly dominated potential energy surface. Broida *et al.*^[17] analyzed its rovibrational population distributions and the kinetic isotope effects by quasiclassical trajectory (QCT) calculations using a semi-empirical LEPS potential energy surface. The study showed that the vibrational excitation is very effective for the reaction and the rotational excitation has an orientational effect. The kinetic isotope effects, and the population of OH, have also been studied by Spencer and Glass^[18] and then by McKendrick *et al.*^[14-15]. McKendrick suggested that the OH product rotational excitation, determined from the repulsive release of energy at configurations away from collinearity, is much higher than the related $O(^3P)$ reactions with alkanes^[19], which is particularly favored by a relatively flat bending potential.

In this paper, a three-dimensional time-dependent quantum wave packet was used to study the effects of initial state excitation of the reagents on reaction probability of the $O(^3P)+HBr$ reaction on a semi-empirical LEPS potential energy surface^[17]. The rate constants, the reaction cross sections and the kinetic isotope effects were also investigated.

Received: January 20, 2005; Revised: March 9, 2005. Correspondent: TANG, Bi-Yu (E-mail: tangbiyu@xtu.edu.cn; Tel: 0732-8292195).

*The Project Supported by Research Foundation of Education Department of Hunan Province(02A012)

1 Theory and methods

The quantum calculations were carried out using time-dependent(TD) quantum wave packet method. The starting point of the TD quantum wave packet method is to solve the TD Schrödinger equation

$$i\hbar \frac{\partial \Psi}{\partial t} = \mathbf{H} \Psi \quad (1)$$

The Hamiltonian expression in the reactant Jacobi coordinate for a given total angular momentum J can be written as

$$\mathbf{H} = -\frac{\hbar^2}{2\mu_R} \frac{\partial^2}{\partial R^2} + \frac{(J-j)^2}{2\mu_R R^2} + \frac{j^2}{2\mu_r r^2} + V(r, R) + \mathbf{h}(r) \quad (2)$$

where r and R are the vibrational and the translational vectors, μ_r and μ_R are the corresponding reduced mass, J and j represent the total angular momentum operator and rotational angular momentum operator of HBr, respectively; $\mathbf{h}(r)$, the diatomic reference Hamiltonian, is defined as

$$\mathbf{h}(r) = -\frac{\hbar^2}{2\mu_r} \frac{\partial^2}{\partial r^2} + V_r(r) \quad (3)$$

where $V_r(r)$ is a diatomic reference potential.

The TD wave function satisfying the Schrödinger equation can be expanded in terms of the body-fixed translational-vibrational-rotational basis defined by using the reactant Jacobi coordinate as^[20]

$$\Psi_{\nu_0 j_0 k_0}^{JM\epsilon}(R, r, t) = \sum_{n v j k} F_{n v j k, \nu_0 j_0 k_0}^{JM\epsilon}(t) u_n^v(R) \Phi_{v, j}(r) Y_{j k}^{JM\epsilon}(R, r) \quad (4)$$

where n is the translational basis label, while M and K are the projection quantum numbers of J on the space-fixed z axis and body-fixed z axis, respectively. (ν_0, j_0, k_0) denote the initial rovibrational state, and ϵ is the parity of the system defined as $\epsilon = (-1)^{J+L}$, with L being the orbital angular momentum quantum number. The detailed definition of various basis functions can be found in Ref.[20].

The split-operator method^[21] is employed to carry out the wave packet propagation

$$\Psi^{JM\epsilon}(R, r, t+\Delta) = e^{-i\mathbf{H}_0\Delta/2} e^{-i\mathbf{U}\Delta} e^{-i\mathbf{H}_0\Delta/2} \Psi^{JM\epsilon}(R, r, t) \quad (5)$$

where the reference Hamiltonian \mathbf{H}_0 is defined as

$$\mathbf{H}_0 = -\frac{\hbar^2}{2\mu_R} \frac{\partial^2}{\partial R^2} + \mathbf{h}(r) \quad (6)$$

and the effective potential operator \mathbf{U} is defined as

$$\mathbf{U} = \frac{(J-j)^2}{2\mu_R R^2} + \frac{j^2}{2\mu_r r^2} + V(R, r) = V_{\text{rot}} + V \quad (7)$$

the matrix version for the expansion coefficient vector F is then given by

$$F(t+\Delta) = e^{-i\mathbf{H}_0\Delta/2} e^{-i\mathbf{U}\Delta} e^{-i\mathbf{H}_0\Delta/2} F(t) \quad (8)$$

where the operator $e^{-i\mathbf{U}\Delta}$ is further split as

$$e^{-i\mathbf{U}\Delta} = e^{-iV_{\text{rot}}\Delta/2} e^{-iV\Delta} e^{-iV_{\text{rot}}\Delta/2} \quad (9)$$

In which V_{rot} is diagonal in the angular momentum representation, and V is diagonal in the coordinate representation. The time-dependent wave function is absorbed at the edges of the grid to avoid boundary reflection^[22]. Finally, the initial state-selected total reaction probabilities are obtained through the flux calculation

$$P_i^r(E) = \frac{\hbar}{\mu_r} \text{Im} \left| \langle \Psi_{iE}^+ | \delta(r-r_0) \frac{\partial}{\partial r} | \Psi_{iE}^+ \rangle \right| \quad (10)$$

The stationary wave function Ψ_{iE}^+ is obtained through a Fourier transform, as described in Ref.[20].

After the reaction probabilities $P^J(E)$ have been calculated for all fixed angular momentum J , the reaction cross sections for a specific initial state could be evaluated by simply summing the reaction probabilities over all the partial waves (total angular momentum J)

$$\sigma_{\nu_0 j_0}(E) = (\pi/k_{\nu_0 j_0}^2) \sum_J (2J+1) P_{\nu_0 j_0}^J \quad (11)$$

$k_{\nu_0 j_0}$ is the wave number, which corresponds to the initial state at fixed collision energy E .

The corresponding specific rate constants $k(T)$ can be calculated by thermally averaging the collision energy of the cross sections $\sigma_{\nu_0 j_0}(E)$ as Ref.[23]

$$k(T) = \left(\frac{8k_B T}{\pi \mu_R} \right)^{1/2} (k_B T)^{-2} \int_0^\infty E \sigma(E) \exp\left(-\frac{E}{k_B T}\right) dE \quad (12)$$

Where k_B is the Boltzmann constant and E is the collision energy.

2 Results and discussion

2.1 Numerical aspect

Extensive convergence tests have been performed with respect to the computational parameters in order to determine the optimum values. The parameters, which are to be adjusted, include the grid sizes, position and width of the initial wave packet (IWP), time step, total propagation time and the absorption parameters. These tests were performed mainly with the $J=0$ partial wave. The parameters finally employed are as follows: the translational coordinate R extends from $R_1=0.5a_0$ to $R_4=13a_0$, the interaction region is defined within R_1 and $R_2=8a_0$, IWP is launched at $R_3=10a_0$ and the width of it is taken to be 0.20 a.u. In calculations, one wave packet is enough to generate convergent reaction probabilities for the energy range of interest. The

absorption region on the reactant side starts from the position that is a little bit larger than R_s . Because the mass center of HBr is close to the Br atom and the O-Br interaction is quite repulsive, we are able to choose a larger value of the vibrational coordinate r which extends from $r_1=0.5a_0$ to $r_3=10a_0$. The dividing surface for flux calculation is located at $r_2=6a_0$ and the absorption begins from r_2 to r_3 . A total of 180 translational bases functions are used to expand the wave function in the interaction region. 100 vibrational and 70 rotational bases functions are used in the expansion of the wave function, a time step of 10 a.u is taken to propagate the wave packet.

As a representative of the convergence tests, Fig.1 presents reaction probabilities from two different numbers of translational bases while all other parameters are kept the same. The solid line is for 180 translational bases and the open circle is for 200 bases. The two results are almost indistinguishable. This means that 180 translational bases are large enough to yield a converged result.

2.2 Reaction probabilities

Fig.2a shows the calculated total reaction probabilities as a function of collision energy from the ground state of HBr at zero total angular momentum $J=0$. As can be seen from Fig.2a, there are two local maxima in the curve: the first one locates at the energy of about 0.12 eV, and the other locates at the energy of about 0.22 eV. We know that there is a $13.22 \text{ kJ} \cdot \text{mol}^{-1}$ (about 0.14 eV)^[17] barrier on the reaction system PES. Furthermore, there is atom hydrogen transfer between two relatively heavy atoms bromine and oxygen in the reaction. So the first local maximum maybe results from tunneling effect. The reason for another local maximum in the curve may be associated with other features of the reactive system such as small skew angle (15.6°

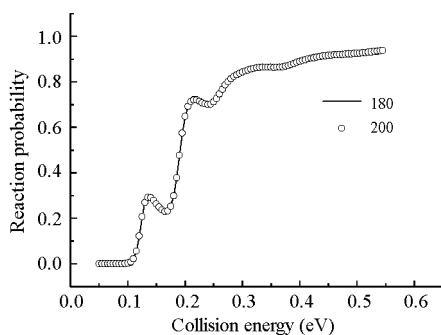


Fig.1 Comparison of the $J=0$ reaction probability results at 25000 a.u propagation time between two parameter sets
Solid line is for 180 translational bases and open circle is for 200 translational bases. Other parameters are the same as described in the text.

for O+HBr, and 21.4° for O+DBr)^[1,17]. The small skew angle may serve to trap 'trajectories' at small reactant separations and promote a resonance phenomenon. In Fig.2a, it also shows that the probabilities begin to increase from zero when the collision energy is larger than 0.10 eV. So the reaction occurs with an essentially non-zero threshold energy of about 0.10 eV. This is corresponding to the $13.22 \text{ kJ} \cdot \text{mol}^{-1}$ barrier of the PES^[17].

In order to investigate the influence of excitation of the reagent on reaction dynamics, some reaction probabilities for excited vibrational and rotational states were also calculated. The energy-resolved reaction probabilities with HBr initially in rovibrational states ($\nu=1,2,3, j=0$) are shown in Fig.2. It is clear that the reaction probabilities significantly increase at low collision energy for the vibrational excitation of HBr, which indicates that the vibrational energy is effective for the reaction. It is also shown that with the vibration quantum number increases, the essentially non-zero threshold energy of the reaction becomes lower ($\nu=1$), even diminishes ($\nu \geq 2$).

Further calculations show that the probabilities, in generally, become small with increasing the rotation quantum number j , as shown in Fig.3. However, for some small rotation quantum number j , the reaction probabilities of some states exceed $j=0$ probabilities in definite collision energy range (it is about 0.12~0.18 eV for $j=1$; 0.14~0.18 eV for $j=2$). The influence of rotation on reactivity is usually discussed on the basis of an orientational effect and an energetic effect, taking into consideration of the topography of the potential energy surface^[24-31]. The orientational effect, which is mainly important for low values of j , usually causes a decline in reactivity with j increases, due to disruption of the favorable orientation to reaction (usually collinear).

However, under certain conditions, rotation may be helpful

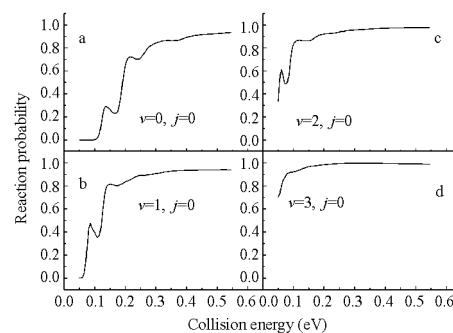


Fig.2 Total reaction probabilities as a function of collision energy for the reaction O+HBr for total angular momentum $J=0$ computed at different vibration states

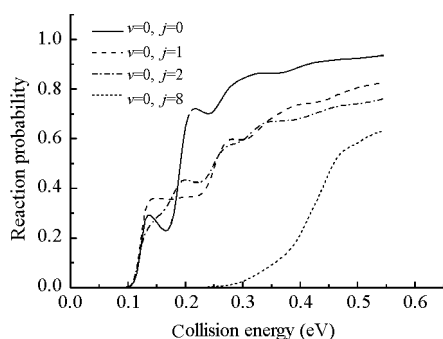


Fig.3 Total reaction probabilities as a function of collision energy for the reaction $O+HBr$ for total angular momentum $J=0$ computed at different rotation states

to achieve the favorable orientation, and no decline will occur. For this to happen, it is required that the barrier will not increase steeply with the deviation from collinearity^[17]. Moreover, rotational energy may become available to surmount the barrier due to the extension of the bond of the rotating molecule through vibration-rotation interaction^[25,28-31]. In such a situation, reactivity will be enhanced when j is increased.

2.3 Integral cross sections and rate constants

The integral cross sections for the title reaction at the initial ground state of HBr have also been calculated. As shown in Fig.4, it is clearly shown that the integral cross sections have energy threshold. This is consistent well with the PES and probabilities curves. With the increase of reagent kinetic energy, the cross sections display a large increase.

The temperature dependent thermal rate constants $k(T)$ from 200 K to 550 K were calculated. The calculated rate constants for $O+HBr(v=0, j=0)$, as well as experimental results^[24] are plotted on a semilogarithmic scale as a function of T^{-1} in Fig.5. It can be seen that, in general, the calculated results are consistent with the experimental results at the considered temperature range. Although the spin-orbit coupling is not considered here,

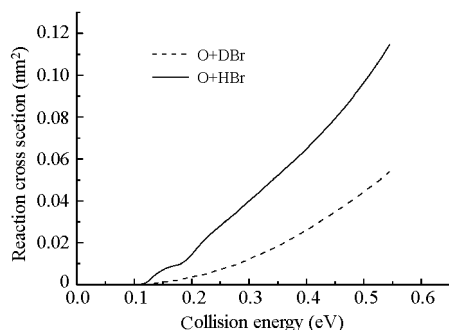


Fig.4 Reaction cross sections as a function of collision energy

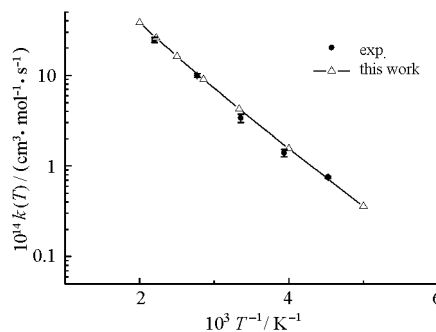


Fig.5 Semilogarithmic plots of rate constants $k(T)$ as a function of T^{-1} for the reaction $O(^3P)+HBr \rightarrow HO+Br$ present quantum calculation results ($-\Delta-$), experimental results of Nava, Basco and Stief (\bullet)^[24]

this consistency implies that this spin-orbit coupling might not be very important for the rate constants in the $O(^3P)$ reaction systems.

2.4 O+DBr reaction and kinetic isotope effects

The same calculations for the isotope reaction $O+DBr \rightarrow OD+Br$ were also carried out. With the substitution of light atom H by heavy atom D and the changing of skew angle ($15.6^\circ \sim 21.4^\circ$), it will lead to a little different kinetic feature between $O+HBr$ and $O+DBr$ reactions. The different features can be reflected in Fig.6 and Fig.7, which display the reaction probabilities as a function of collision energy for various vibrational excited states and rotational excited states. In Fig.6, as the relative heavy atom D replaces the original light atom H , the increase of reaction probability with energy becomes slow and the amplitude of the local maximum becomes relatively small comparing with Fig.2. In Fig.7, it can be seen that in some energy range for some low rotational excitation, energy range of reactivity enhancement by rotational excitation becomes wider and the reaction probabilities

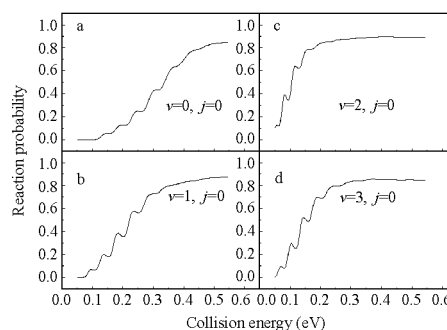


Fig.6 Total reaction probabilities as a function of collision energy for the reaction $O(^3P)+DBr$ for total angular momentum $J=0$ computed at different vibration states

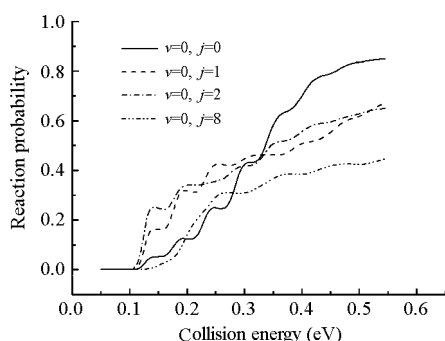


Fig.7 Total reaction probabilities as a function of collision energy for the reaction $O(^3P) + DBr$ for total angular momentum $J=0$ computed at different vibration states

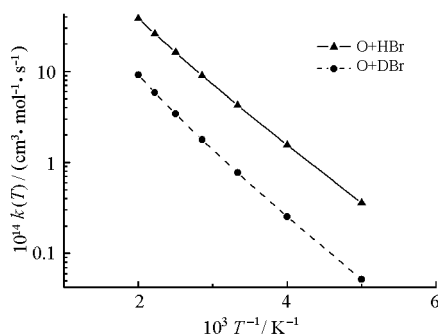


Fig.8 Semilogarithmic plots of rate constants $k(T)$ as a function of T^{-1}

increase more obviously.

Reaction cross sections of $O+DBr$ reaction were calculated in the energy range from 0.05 eV to 0.55 eV as shown in Fig.4. As can be seen from Fig.4, the values of $O+DBr$ are always smaller than the corresponding values of $O+HBr$; this characteristic can also be reflected by comparison of the probabilities curves between Fig.2 and Fig.6. Rate constants k_{O+DBr} , calculated from the cross sections are plotted as a function of T^{-1} in Fig.8. In order to study kinetic isotope effects, the results of k_{O+HBr} were also plotted in Fig.8. As can be seen from Fig.8, rate constants k_{O+DBr} are also always smaller than k_{O+HBr} , and the two curves are approximately parallel. So the kinetic isotope effects in the reaction system are relatively obvious.

3 Conclusions

The reaction dynamics for the $O(^3P) + HBr(DBr)$ reaction has been studied using the accurate full three-dimensional quantum wave packet method on a semi-empirical LEPS potential energy surface. The calculations showed that the reaction would occur with essentially non-zero threshold energy, and initial vibra-

tional excitation of reagents leads generally to increase of the total reaction probabilities, which can be understood as “corner cutting”^[32] or seen in a different way as the opening up of the cone of acceptance for reaction upon vibrational excitation^[33]. In some energy range low level of rotational excitation exhibits somewhat orientational effect, probably mainly due to the extension of the H—Br bond through vibration-rotation interaction. The cross sections are also calculated, which show energy threshold. At the considered temperature range, the calculated rate constants are consistent with the experimental results. With the changing of atom mass and skew angle, the reaction $O+HBr$ has relative obvious kinetic isotopic effects, such as the difference in probabilities, cross sections and rate constants.

References

- Levine, R. D.; Bernstein, R. B. *Molecular reaction dynamics and chemical reactivity*. Oxford: Oxford University Press, 1987: 170
- Whitely, T. W. J.; Dobbyn, A. J.; Connor, J. N. L.; Schatz, G. C. *Phys. Chem. Chem. Phys.*, **2000**, **2**: 549; Sokolovski, D.; Connor, J. N. L.; Schatz, G. C. *J. Chem. Phys.*, **1995**, **103**: 5979
- Skodje, R. T.; Skouteris, D.; Manolopoulos, D. E.; Lee, S. H.; Dong, F.; Liu, K. *Phys. Rev. Lett.*, **2000**, **85**: 1206
- Skokov, S.; Tsuchida, T.; Nanbu, S.; Bowman, J. M.; Gray, S. K. *J. Chem. Phys.*, **2000**, **113**: 227
- Noda, S.; Demise, H.; Claesson, O.; Yoshida, H. *J. Phys. Chem.*, **1984**, **88**: 2552
- Nobusada, K.; Nakamura, H.; Lin, Y.; Ramachandran, B. *J. Chem. Phys.*, **2000**, **113**: 1018; Aoiz, F. J.; Banares, L.; Castillo, J. F.; Menendez, M.; Verdasco, J. E. *Phys. Chem. Chem. Phys.*, **1999**, **1**: 1149
- Zhang, R.; van der Zande, W. J.; Bronikowski, M. J.; Zare, R. N. *J. Chem. Phys.*, **1991**, **94**: 2704
- Christoffel, K. M.; Bowman, J. M. *J. Chem. Phys.*, **2002**, **116**: 4842
- Xie, T.; Wang, D.; Bowman, J. M.; Manolopoulos, D. E. *J. Chem. Phys.*, **2002**, **116**: 7461
- Xie, T.; Bowman, J. M.; Peterson, K. A.; Ramachandran, B. *J. Chem. Phys.*, **2003**, **119**: 9601
- Martínez, T.; Hernández, M. L.; Alvarinõ, J. M.; Aoiz, F. J.; Rábanos, V. S. *J. Chem. Phys.*, **2003**, **119**: 7871
- Ramachandran, B.; Peterson, K. A. *J. Chem. Phys.*, **2003**, **119**: 9590
- Lin, S. Y.; Han, K. L.; Zhang, J. Z. H. *Phys. Chem. Chem. Phys.*, **2000**, **2**: 2529

- 14 McKendrick, K. G.; Rakestraw, D. J.; Zare, R. N. *Faraday Discussions Chem. Soc.*, **1987**, **84**: 39
- 15 McKendrick, K. G.; Rakestraw, D. J.; Zhang, R.; Zare, R. N. *J. Phys. Chem.*, **1988**, **92**: 5530
- 16 Brouard, M.; Valance, C. *Phys. Chem. Chem. Phys.*, **2001**, **3**: 3602
- 17 Broida, M.; Tamir, M.; Persky, A. *Chem. Phys.*, **1986**, **110**: 83
- 18 Spencer, J. E.; Glass, G. P. *Int. J. Chem. Kinet.*, **1997**, **11**: 97
- 19 Sweeney, G. M.; Watson, A.; McKendrick, K. G. *J. Chem. Phys.*, **1997**, **106**: 9172
- 20 Zhang, D. H.; Zhang, J. Z. H. *J. Chem. Phys.*, **1994**, **101**: 1146
- 21 Fleck, J. A.; Morris, J. R.; Feit, M. D. *Appl. Phys.*, **1976**, **10**: 129
- 22 Neuhauser, D.; Baer, M. *J. Chem. Phys.*, **1989**, **91**: 4651
- 23 Aoiz, F. J.; Bañares, L.; Castillo, J. F. *J. Chem. Phys.* **1999**, **111**: 4013
- 24 Nava, D. F.; Basco, S. R.; Stief, L. J. *J. Chem. Phys.*, **1983**, **78**: 2443
- 25 Persky, A.; Broida, M. *J. Chem. Phys.*, **1984**, **81**: 4352
- 26 Hodgson, B. A.; Polanyi, J. C. *J. Chem. Phys.*, **1971**, **55**: 4745
- 27 Polanyi, J. C.; Schreiber, J. L. *Faraday Discussions Chem. Soc.*, **1977**, **62**: 267
- 28 Polanyi, J. C.; Sathyamurthy, N. *Chem. Phys.*, **1978**, **33**: 287
- 29 Blackwell, B. A.; Polanyi, J. C.; Sloan, J. J. *Chem. Phys.*, **1978**, **30**: 299
- 30 Polanyi, J. C. *Faraday Discussions Chem. Soc.*, **1979**, **67**: 110
- 31 Sathyamurthy, N. *Chem. Rev.*, **1983**, **83**: 601
- 32 Smith, I. W. M. *Kinetics and dynamics of elementary gas reactions.* London: Butterworths Press, 1980
- 33 Schechter, I.; Kosloff, R.; Levine, R. D. *Chem. Phys. Lett.*, **1985**, **121**: 297

O(³P)+HBr(DBr)反应的含时量子散射计算*

左国平^{1,2} 唐璧玉^{1,2} 韩克利³

(¹湘潭大学物理学院, 湖南湘潭 411105; ²湘潭大学现代物理研究所, 湖南湘潭 411105;

³中国科学院大连化学物理研究所, 分子反应动力学国家重点实验室, 辽宁大连 116023)

摘要 基于 LEPS 势能面, 用三维含时量子波包法对 O(³P)+HBr(DBr)反应进行了准确的动力学计算. 计算的结果表明, 振动激发对这个反应是有效的, 而转动激发在某一能量范围内具有方位效应. 计算得到了该反应的速率常数和反应截面, 速率常数 $k_{\text{O+HBr}}$ 的计算值同实验值符合得很好. 通过对相应结果的对比, 可以发现这个反应具有比较明显的同位素效应.

关键词: 含时量子波包法, 速率常数, 反应截面

中图分类号: O641